Ivan A. Reyes, Julie S. Chalfant, Chryssostomos Chryssostomidis
Massachusetts Institute of Technology

Design and Modeling of the Navy Integrated Power and Energy Corridor Cooling System

ABSTRACT

This paper presents a first-pass design of a Navy Integrated Power and Energy Corridor (NiPEC) liquid cooling system. Numerical analysis and computer-based modeling were used to develop an indirect liquid-cooling system suited for use aboard U.S. Navy surface vessels. A review of thermal and fluid dynamic theory, comparisons to existing technologies, and 3D computer-aided design (CAD) simulations provided the test bed for design tradespace exploration. Guided by Department of Defense and industry requirements, a new cooling paradigm was developed which facilitates inter-system operations and provides a robust platform through comprehensive component design. Consideration was given to the cooling system layout and architecture to promote human-system interaction and efficient arrangement within the NiPEC footprint. Documented is the initial investigation, equipment analysis, concept selection, and proof-of-concept testing that set the foundation for future prototyping and NiPEC cooling system development.

1 BACKGROUND

As part of an ongoing U.S. Navy research consortium for next-generation warships, the Design Laboratory of the MIT Sea Grant Program is developing the Navy integrated Power and Energy Corridor (NiPEC) to underpin the vessel's power distribution system. The corridor comprises several modular compartments capable of operating independently or as part of a network to execute energy storage, conversion, protection, control, isolation, and transfer functions. The power conversion process is carried out by the corridor's integrated Power Electronics Building Block (iPEBB). The iPEBB, seen in Fig. 1, is a self-contained universal converter configured to provide power-dense solutions to the ship's stochastic and dynamic loads [1]. The plug-and-play iPEBB is designed to be easily inserted and removed with no adjustments or connections required beyond the insertion/removal and latching. A key challenge with the iPEBB's advanced semiconductor technology is the mitigation of its thermal load, constrained by the prohibition against direct liquid cooling [2]. In response, MIT is exploring the use of liquid cooling with a dry interface; *i.e.*, conductive heat transfer through the surface of the iPEBB via a thermal interface material to liquid-cooled cold plates embedded in the NiPEC.

1.1 Problem Statement

Electrical losses from the internals of the iPEBB generate heat that must be removed to prevent component damage and system degradation. The current design and analysis of the iPEBB assumes a heat load of approximately 10 *kW* and serves as the base assumption for this study. The heat is transmitted and spread through component substrates and the unit's baseplate to the top and bottom faces of the iPEBB. The amount of heat requiring removal is not extreme by current industry standards, but it is complicated by imposed design constraints. First, the iPEBB is prohibited from having any liquid cooling connections. This eliminates the possibility of direct cooling methods, which functionally have a greater thermal capacity. Second, the iPEBB must be compact, lightweight, and resilient to physical damage. This prevents the use of casing fins to dissipate heat to the air and surrounding environment [2]. Third, the unit's anchoring mechanism must interface with the casing's outer surface to secure the unit from static and dynamic forces. The cooling method and anchoring interface must develop an integrated design approach to prevent interference and promote synergistic operations. Lastly, the thermal management solution must conform to industry and military design standards.

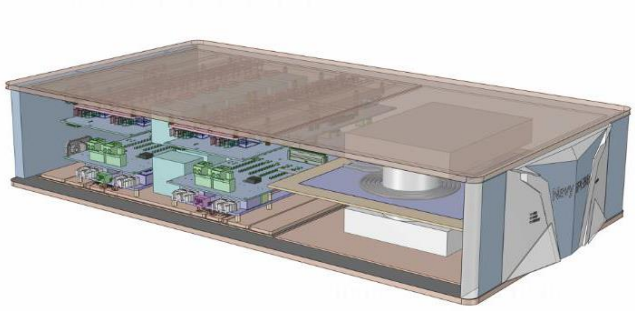

Figure 1. Navy iPEBB, image courtesy of the Virginia Tech Center for Power Electronics Systems.

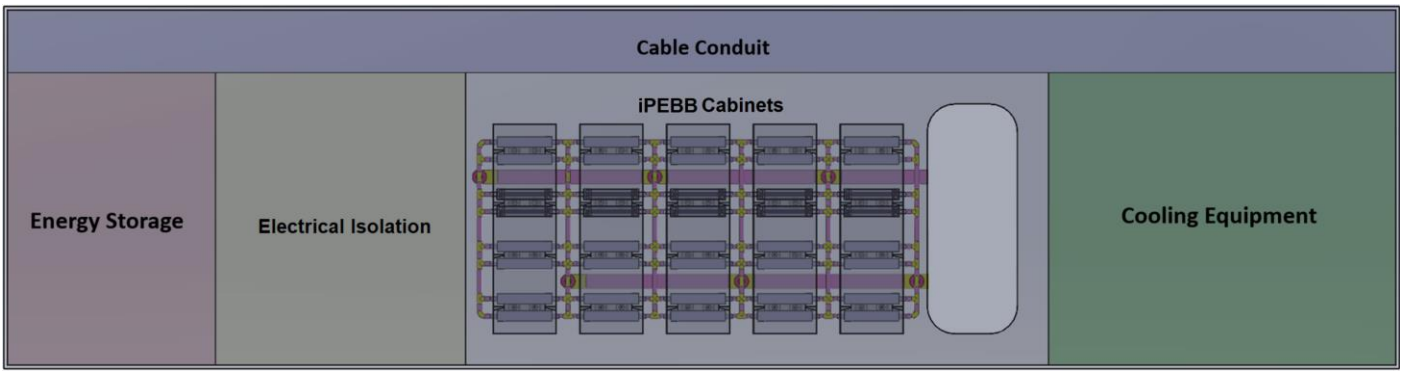

Figure 2. Notional NiPEC compartment.

1.2 Base Assumptions

A four-corridor NiPEC system serves as the base model for assumptions made in this study. Each corridor is comprised of 12 compartments, with each compartment housing 20 iPEBBs. The 20 iPEBBS are distributed into five cabinets which are termed iPEBB stacks. Each iPEBB stack contains four iPEBBs stacked in vertical alignment. Fig. 2 and 3 show an idealized compartment and ship arrangement.

The iPEBB mainly operates in two different load conditions. The first condition assumes an equal heat load distribution across all semi-conductor switches. The second condition assumes that half the switches produce 80% of the heat load and the other half 20% (80/20 condition). Assuming the iPEBB produces 10kW of heat and is designed with 96 switches, the maximum heat load per switch in each condition is 104W at even load and 167W for the 80/20 condition. Therefore, the 80/20 condition is the most thermally limiting situation and serves as the basis for cooling system assumptions and requirements [4].

The remainder of the paper is organized as follows. Section 2 describes the piping system arrangement and pump design. Section 3 details heat exchanger development and fluid simulation. Section 4 discusses expansion tank sizing and operating characteristics. Section 5 explains pipe and fitting selection. Section 6 delineates the use of water chemistry equipment. Section 7 discusses cold plate design iteration. Conclusions and recommendations for future work are presented in Sections 8 and 9.

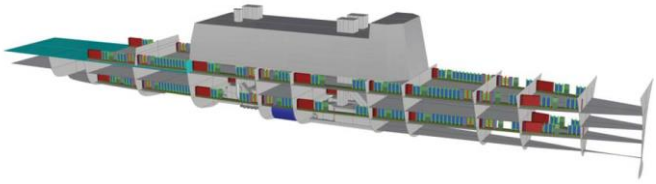

Figure 3. Perspective view of the NiPEC system in the notional ship. © 2022 IEEE. Reprinted, with permission, from [3].

2 COOLING SYSTEM ARCHITECTURE AND PUMP DESIGN

2.1 Base Cooling System Architecture

The notional NiPEC cooling system is a closed-loop, pressurized, demineralized water cooling system. It is comprised of components required to ensure continuous flow and adequate cooling of the iPEBB architecture within the NiPEC compartment. Heat exchangers, pumps, water chemistry control instruments, pipes and fittings, expansion tank, cold plates, and water filters are the major components to be assessed in meeting this goal.

An initial cooling system diagram was developed based on the guidelines provided by [5], and is shown in Fig. 4. Several design iterations were explored over the course of this study and concluded with the diagram presented in Fig. 5. The final system architecture incorporates several military and industry standards that consider construction, maintenance, and operational requirements.

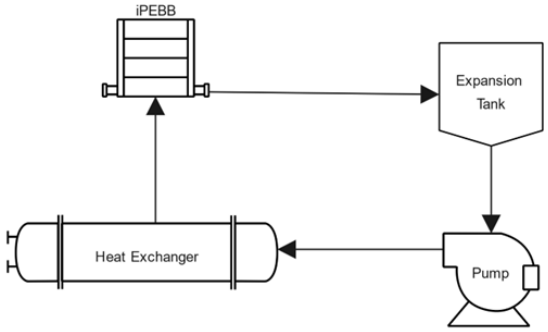

Figure 4. Initial cooling system schematic

Overarching assumptions are based on [7], which provides the requirements for cooling water systems in support of shipboard electronic equipment. Demineralized water is the chosen NiPEC cooling system medium as it eliminates or lessens the risk of electrical conductivity between components and the corrosion of equipment. Cooling system water pressure must be within the operating range of 10 to 110 *lbs/in*^{2} and be capable of withstanding a hydrostatic test pressure of 150 *lbs/in*^{2}. Analysis and modeling assume a 100 *lbs/in*^{2} system operating pressure to mitigate the risk of water contamination from interfacing support systems (*i.e.* heat exhanger tube leakage) at lower pressures.

2.2 Pump Design

The pump component of the NiPEC cooling system provides the motive force for the cooling fluid that ensures continuous flow to the electronic components and through the system. Pumps used in Navy shipboard electronic cooling water systems are centrifugal pumps as they are more efficient at providing large amounts of flow to fluids at lower viscosities. They are typically simpler in design, more compact, and less difficult to maintain than positive displacement pumps. The centrifugal pump's design enables the operator to more readily adjust system flow and pressure characteristics. Therefore, all calculations and assumptions for the notional NiPEC cooling system utilize centrifugal pumps to provide system flow.

Based on the assumptions made by [8] for equipment allocation and vertical spatial allowances, five iPEBB stacks, each consisting of four iPEBBs would optimally fit within the footprint of the model NiPEC. At a 10 *kW* per iPEBB heat load and a 20% safety margin, the idealized compartment would require a cooling system capable of dissipating 240 *kW* of heat.

The maximum volumetric flow rate for a shipboard cooling water system must be adjusted to 1.4 gallons per minute per kilowatt load and a maximum rise in water temperature of 2$^{\circ}C$ [7]. Therefore, for a 240 *kW* load, the required maximum volumetric flow rate is 336 *gpm*. As the pump takes suction directly from the system's expansion tank, it is assumed that the demineralized water enters the pump at a maximum temperature of 46 °C based on the assumptions in Section 3.

In determining the total dynamic head of the cooling system, frictional losses from system equipment, fittings, and piping were considered. The piping run with the greatest anticipated pump head was used for calculations as it presented the most conservative approach. The chemical resin bed and micron filter components are not in-line with the main cooling path and were therefore not directly incorporated into the total dynamic head calculation. The pump suction filter is a y-strainer with expected pressure losses equivalent to commercially available products of the same design. The iPEBB stack and heat exchanger losses were assumed to be the maximum permissible values allowed by standards [7,9].

Piping frictional losses were calculated using the Darcy-Weisbach equation,

$$\Delta p = f_D \frac{L}{D} \frac{\rho}{2} (v)^2 \qquad (1)$$

where f_D is the Darcy friction factor, L is the length of the pipe, D is the internal diameter of the pipe, ρ is the density of the fluid and v is the mean flow velocity.

The diameters for the supply and return header piping were assumed to be 3.5 *in* and 4 *in*, respectively. Piping branches off the main headers that provide cooling to and from individual cold plate branches were determined to be 2 *in* in diameter. A 1 *in* diameter pipe was used for the inlet and outlet branches providing cooling to individual cold plates. The piping sizes were derived by the safe flow velocities determined in Section 5, the thermal properties of the demineralized water, a total maximum volumetric flow rate of 336 *gpm*, and the continuity of mass equation. The pipe lengths were derived from NiPEC cooling system CAD modeling based on the compartment geometric allowances documented by [8]. The Darcy Friction Factor was calculated using

$$f_D = (0.79 \ln(Re) - 1.64)^{-2} \qquad (2)$$

where *Re*, Reynolds number, values were based on the selected piping diameter and thermal properties of water.

Fitting frictional losses, h_L, were calculated using a derivation of Eqn. (1) for dimensional analysis using resistance coefficients [10].

$$h_L = K \frac{v^2}{2g} \qquad (3)$$

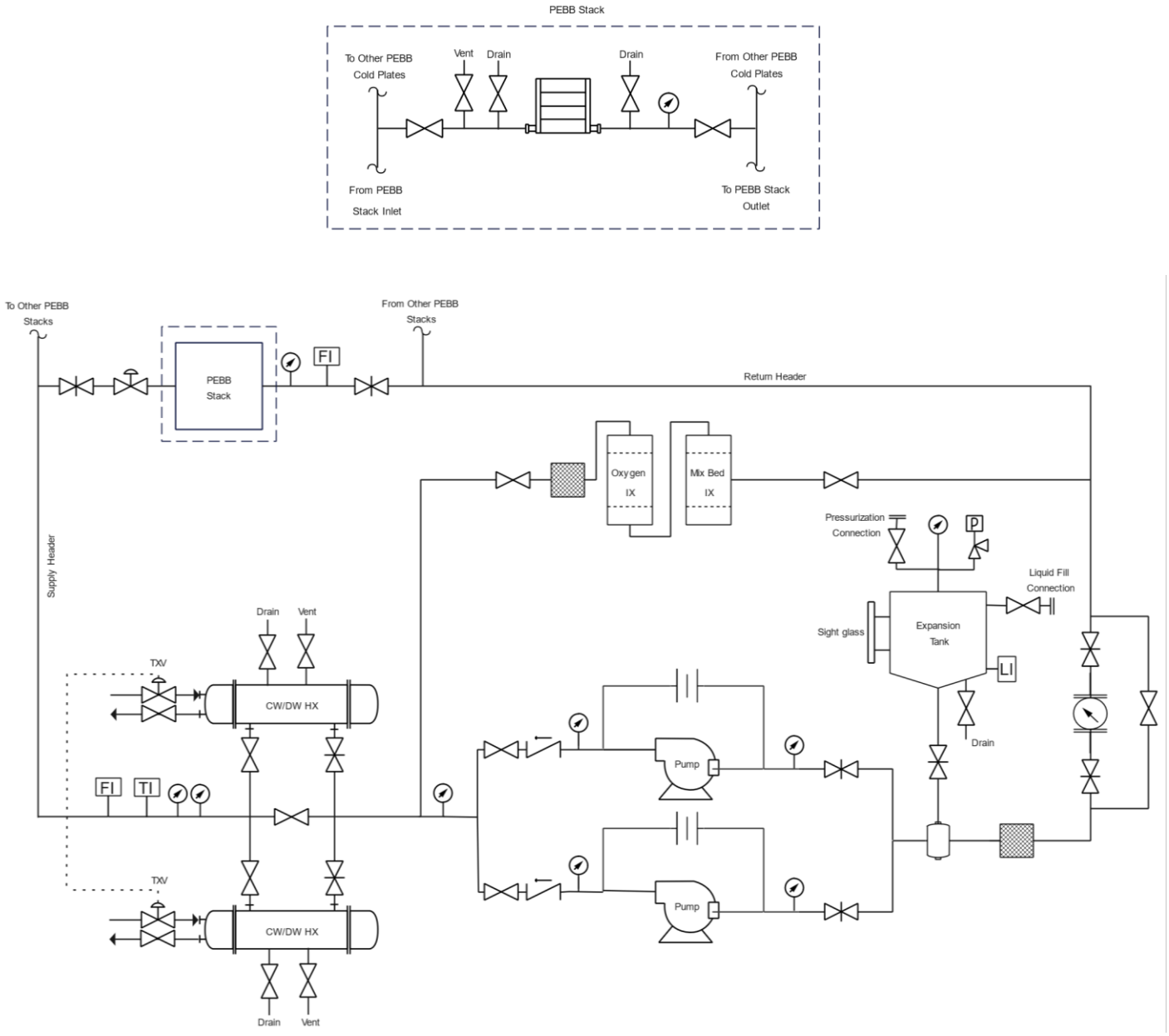

Figure 5. Final cooling system schematic [6].

where K is the resistance coefficient, and g is the gravitational acceleration. Fitting type, quantity, and allocation were based on the requirements that developed Fig. 5 [6].

Typical pump efficiencies for small AC-powered centrifugal pumps range between 55% and 71%. Centrifugal pumps operate with higher efficiencies when supplying maximum volumetric flow against a relatively benign pump head. A pump efficiency of 70% was chosen based on the calculated total dynamic pump head at maximum flow. The selected pump efficiency was validated by comparison to the efficiencies of similar commercially available pumps. The power required by the pump was calculated using the pump power equation

$$P = \frac{\dot{V}\rho g(TDH)}{\eta} \qquad (4)$$

where P is the pump power (kW), $\dot{V}$ is the volumetric flow rate, TDH is the total dynamic head, and η is the pump efficiency. The required pump power is calculated to be 16.21 kW or 21.87 hp.

3 HEAT EXCHANGER DESIGN AND FLUID SIMULATION

Heat exchangers used in Navy shipboard electronic cooling water systems are either plate-type or shell-and-tube coolers. A shell-and-tube heat exchanger design was used as they are capable of operating with higher system temperatures and pressures, produce a smaller pressure loss across the heat exchanger, enable easier leak identification and repair, require less complicated maintenance, and are less prone to physical damage.

3.1 Heat Exchanger Theory and Design

Determining the appropriate design criteria and geometries for the cooling system heat exchanger requires the calculation and iteration of heat transfer variables and their conformance to standards. The subsequent calculations follow the derivations of [11] and [12]. A derivation of Fourier's Law, Eqn. (5), for multi-composite structures is the fundamental equation used to characterize the heat exchanger design and required heat transfer surface area.

$$Q^{\cdot} = UA\Delta T \qquad (5)$$

where $\dot{Q}$ is the rate of heat transfer, U is the overall heat transfer coefficient, A is the external surface area for the tube bundle, and ΔT is the log mean temperature difference. Individual material and fluid heat transfer coefficients were calculated ahead of determining the overall heat transfer coefficient as detailed by [6].

Applying the definition of the Overall Heat Transfer Coefficient from [12], Eqn. (5) is rewritten:

$$U = \frac{\dot{Q}}{A\Delta T} = \frac{1}{\frac{1}{h_{CW}} + \frac{L}{k} + \frac{1}{h_{DI}}} \qquad (6)$$

where h_{DI} is the ideal heat transfer coefficient for the demineralized water derived by the Bell Delaware Method, h_{CW} is the ideal heat transfer coefficient for the chilled water determined by heat balance calculations, L is the thickness of the tube, and k is the thermal conductivity of the tube material. Per [9], the tubes are assumed to have an outside diameter of 0.375 *in*, a wall thickness of 0.035 *in*, and a thermal conductivity for CuNi 90/10. A fouling resistance is incorporated into the calculation as required by [9].

The log mean temperature difference is calculated by

$$\Delta T = \frac{(T_{hin} - T_{cout}) - (T_{hout} - T_{cin})}{\ln\left(\frac{T_{hin} - T_{cout}}{T_{hout} - T_{cin}}\right)} \qquad (7)$$

where T_{hin} is the demineralized water temperature entering the heat exchanger, T_{hout} is the demineralized water temperature leaving the heat exchanger, T_{cin} is the chilled water temperature entering the heat exchanger, and T_{cout} is the chilled water temperature leaving the heat exchanger.

T_{hout} is $46^{\circ}C$ and T_{hin} is $44^{\circ}C$ based on expected demineralized water temperatures of a iPEBB operating in the 80/20 condition. Using the methodology of [4], the temperature rise from semi-conductor to cooling liquid is determined by

$$Q^{\cdot} = \Delta T_{Net}/R_{Tot} \qquad (8)$$

where ΔT_{Net} is the temperature difference between the semi-conductor switch and cooling water and R_{Tot} is the total thermal resistance from the semi-conductor switch to cooling water.

Using the R_{Tot} calculated by [4] and a $Q^{\cdot}$ of $167W$ per semi-conductor, the ΔT_{Net} is 101.3°C. The maximum component temperature to prevent damage to the iPEBB semi-conductors is 180°C. Using a 30°C safety margin criteria, a 150°C upper-temperature limit is defined. Using the calculated ΔT_{Net} and 150°C limit, the maximum permissible coolant temperature passing through the cold plate is 46°C. Furthermore, the expected coolant temperature difference across the cold plate is assumed to be 2°C based on the requirements of [7]. Therefore, a maximum cold plate coolant inlet temperature of $44^{\circ}C$ is assumed for the heat exchanger's demineralized coolant outlet temperature.

T_{cin} is $7^{\circ}C$ based on expected chilled water system temperatures, and T_{cout} is $27^{\circ}C$. T_{cout} was calculated using the expected thermal heat load of the 20 iPEBBs, a 45 *gpm* flow rate, and the thermal properties of the chilled water.

Finally, utilizing Eqn. (5) and previously derived factors, the required heat exchanger shell-side tube surface area is 7.42 m^2.

3.2 Heat Exchanger Design Criteria and Simulation

Two-pass and four-pass demineralized water heat exchangers were modeled using SOLIDWORKS and its supplemental Flow Simulation software. Cooler geometry and arrangement are based on previous calculations and the design requirements of [9]. A summary of the heat exchanger geometries is listed in Table 1.

The exposed tube length was calculated based on the required surface area, the number of first-pass tubes that could be accommodated on the tube sheet face, and the outside circumference of the 3⁄8 *in* tube. Tube outside

diameters and wall thickness are limited to those listed in Table 2. The tube size restriction is based on preventing tube cracking, erosion-corrosion, flow-induced vibrations, and damage from external vibrations and shock. The tube sheet design assumed the use of inlet-end flared tubes. The tube sheet thickness was not to be less than the depth of expansion, plus the depth of flare, plus 1⁄8 *in*; 0.5 *in* and 0.376 *in* respectively for a 3⁄8 *in* tube. A U-tube design heat exchanger was not chosen due to the complexity of maintenance. A U-tube design requires the tube bundle to be removable and have a floating tube sheet for its back-end support. A straight tube design allows for a fixed tube sheet and the performance of maintenance without the removal of the tube sheet. In regards to the heat exchanger's baffles, alternating top and bottom semicircle baffles rising up to the heat exchanger's centerline were used in the design.

Table 1. Heat exchanger model geometries

Geometry	Two-Pass Model	Four-Pass Model
Waterbox head depth	4 *in*	7 *in*
Exposed tube length	66 *in*	50 *in*
Tube sheet thickness	1 *in*	1 *in*
Overall heat exchanger length	76 *in*	66 *in*
Heat exchanger internal shell radius	4 *in*	7 *in*
Tube spacing (centerline-to-centerline)	0.5 *in*	0.65 *in*
Total number of tubes	148	296
Number of first-pass tubes	74	74
Baffle thickness	0.125 *in*	0.125 *in*
Baffle spacing	4 *in*	6 *in*

The heat exchanger is designed to the flow requirements of [9]. The allowable pressure drops across the heat exchanger for both the cooling and cooled fluid must not exceed 6 lbf/in^2. Cooling water velocities for the chilled water shall not exceed 9 *ft/s* through the heat exchanger tubes and 11 *ft/s* through the heat exchanger inlet piping. Assuming a 45 *gpm* chilled water flow rate, a velocity limit of 11 *ft/s*, and the continuity equation for mass, a 1.5 *in* pipe diameter was chosen for the chilled water inlet and outlet piping. Using the same equation and similar assumptions, an expected tube velocity of 2.67 *ft/s* for 3⁄8 *in* tubes is calculated.

Table 2. Required tube outside diameter and thickness

Outside Diameter	Minimum Wall Thickness
5/8 *in*	0.049 *in*
1/2 *in*	0.049 *in*
3/8 *in*	0.035 *in*

Models were constructed, and a fluid simulation was performed on the two-pass and four-pass heat exchangers. The simulation assumed a chilled water inlet pressure of 100lbf/in^2 and a mass flow rate of 2.893 *kg/s*, or 45 *gpm* at 27°*C*. A second simulation was performed for the demineralized water portion of the heat exchanger. The simulation assumed an inlet pressure of 100 lbf/in^2 and a mass flow rate of 20.9829 *kg/s*, or 336 *gpm* at 46 °*C*.

3.2.1 Two-pass Heat Exchanger Model

Flow trajectories and pressure gradients for chilled water in the two-pass model are shown in Fig. 6. A tubeside pressure drop of approximately 11.7371 lbf/in^2 is calculated from the simulation and does not meet the required design criteria of (6 lbf/in^2). The simulation for velocity gradients calculated that neither the 11 *ft/s* (3.3528 *m/s*) for the chilled water inlet piping or the 9 *ft/s* (2.7432 *m/s*) for the tubes is expected to be exceeded.

Flow trajectories and pressure gradients for demineralized water in the two-pass model are shown in Fig. 7. A shell-side pressure drop of approximately 29.5810 lbf/in^2 is calculated from the simulation and does not meet the required design criteria of 6 lbf/in^2. The demineralized water simulation calculated that velocity gradients are projected to marginally be within the safe limits for the heat exchanger's internal components. A limit of 3.5 *m/s* is derived given the heat exchanger's diameter and material selection of copper-nickel.

3.2.2 Four-pass Heat Exchanger Model

The heat exchanger's geometries were modified to achieve a shell-side tube surface area capable of handling the assumed heat load. The number of first-pass tubes and the tube diameter were unchanged to remain within the required flow velocities. The tube and baffle spacing were increased to lower the demineralized water pressure drop across the heat exchanger. Flow trajectories and pressure gradients for chilled water in the four-pass model are shown in Fig. 8. A tube-side pressure drop of approximately 27.39 lbf/in^2 is calculated from the simulation and does not meet the required design criteria. The simulation for velocity

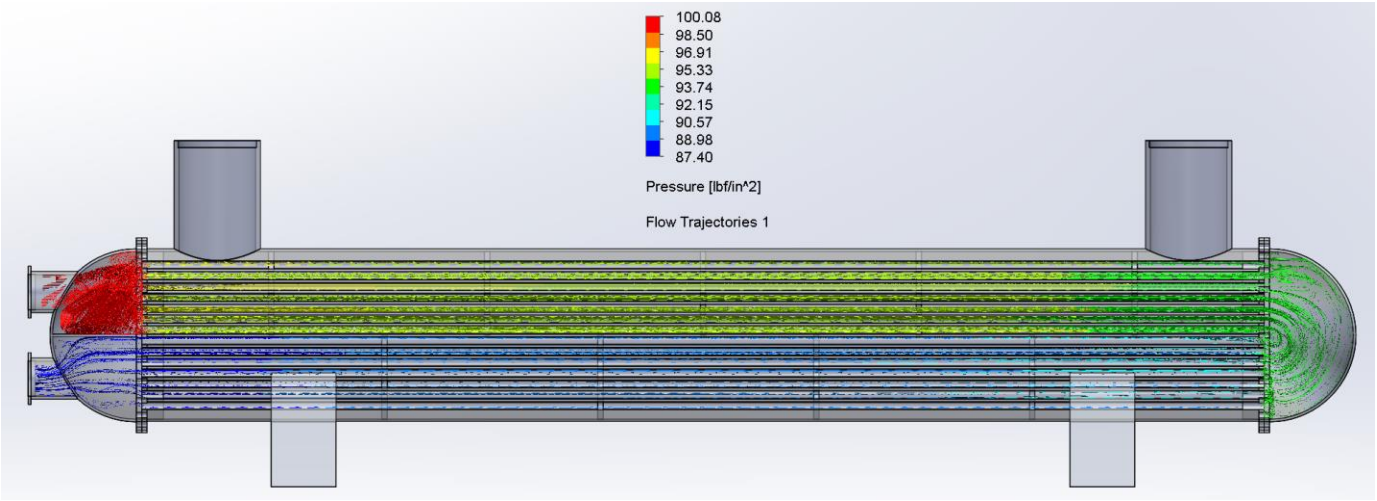

Figure 6. Two-pass heat exchanger chilled water flow pressures.

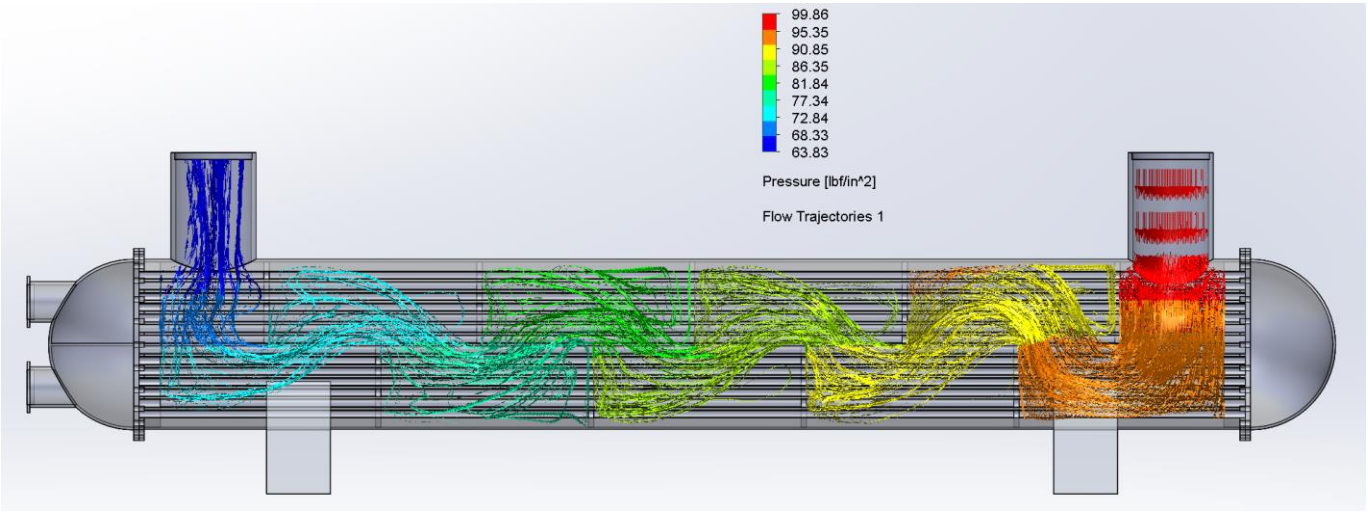

Figure 7. Two-pass heat exchanger demineralized water flow pressures.

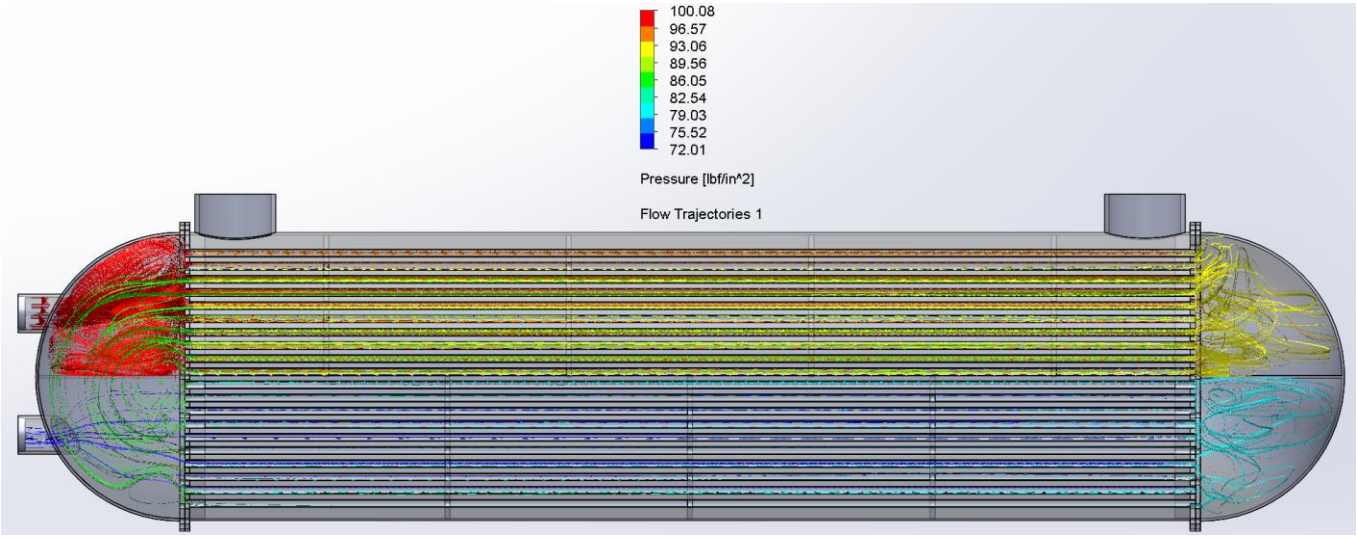

Figure 8. Four-pass heat exchanger chilled water flow pressures.

gradients calculated that the flow velocity criteria is not expected to be exceeded.

A shell-side pressure drop of approximately (5.5323 lbf/in^2) is calculated and meets the required design criteria. The demineralized water simulation calculates that flow velocities are projected to be well within the safe limits for the heat exchanger's internal components.

3.2.3 Heat Exchanger Modeling Conclusions

The two-pass heat exchanger model resulted in lower chilled water pressure losses. The smaller pressure drop was primarily due to having fewer passes for the same number of first-pass tubes as compared to the four-pass heat exchanger. A disadvantage to this model was the pressure drop on the shell-side of the heat exchanger for the demineralized water. The larger pressure drop is attributed to having a smaller internal shell diameter and more closely spaced baffles. However, a more compact baffle arrangement provides greater heat transfer capability to the heat exchanger. The two-pass heat exchanger is 10 *in* longer than the four-pass model in order to maintain sufficient exposed tube surface area for heat transfer. Both heat exchangers have approximately the same heat load capability of 240 *kW* given the differences in their design.

Based on the simulation results, all flow requirements were met by the four-pass heat exchanger, with the exception of the chilled water pressure drop. It is recommended that further heat exchanger optimization is performed to determine the solution that meets all requirements. Modifying the four-pass heat exchanger to a two-pass design with 1⁄2 *in* or 5⁄8 *in* diameter tubes should be pursued. The number of first-pass tubes should scale with the tube diameter in order to maintain a safe but sufficient fluid flow velocity.

4 EXPANSION TANK SIZING

The expansion tank shall be sized to accommodate the thermal expansion of the system coolant, a conservative operating volume, and sufficient safety margins. The thermal expansion volume is based on a cooling water temperature range from 0 to 79 °C, where 0 °C is the minimum phase temperature, and 79 °C is based on the maximum possible temperature seen by the liquid. When the iPEBB operates in the limiting condition described in Section 1.2 and assumes a 180 °C maximum semiconductor temperature, a maximum cooling water temperature of 79 °C is calculated using Eqn. (8).

The volume required for expansion of the liquid in the system considers only the cooling water in the piping and components. Based on model estimated system volumes, a total system volume of 200 gallons is derived. The 200 gallons assumes two heat exchangers, two pumps, two demineralizers, approximately 25 meters of varying pipe sizes, and 40 cold plates. The volume required to accommodate the thermal expansion of the demineralized water was calculated using

$$\Delta V_E = V_\theta \beta \Delta T_{Range} \qquad (9)$$

where ΔV_E is the change in cooling volume due to thermal effects, V_θ is the initial volume of cooling water within the system, β is the volumetric temperature expansion coefficient of water, and ΔT_{Range} is the possible difference of cooling water temperature range. Assuming the value of β is $6.21 \cdot 10^{-4}$ at its most limiting temperature, the required expansion volume is 9.81 gallons.

Typically, the operational volume allowance (V_O) used in determining the total expansion tank volume is based on the need to fill portions of the system from a shutdown condition. The criteria prevents having to refill and check the chemistry of the added water multiple times to fill the system's limiting component (*i.e.* the heat exchanger). As the NiPEC compartment cooling system is not expected to be shut down on a frequent basis, the heat exchanger does not serve as the basis for this volume. V_O is assumed to be 4 gallons and is based on having to fill and restore a single iPEBB stack from a maintenance condition.

A low-level tank margin of 20% total volume is applied to ensure that operators can take timely action to diagnose and restore expansion tank pressure and level conditions. If tank level and pressure were not promptly restored, cavitation and/or air-binding of the pump could occur, leading to loss of flow and cooling to the iPEBBs. A high-level tank margin of 10% total volume is applied as a buffer to prevent the inadvertent wetting of equipment at the top of the tank not intended to come in contact with water.

The total liquid volume of the expansion tank is therefore

$$V_{Tot} = 0.1V_{Tot} + V_E + V_O + 0.2V_{Tot} \qquad (10)$$

where V_{Tot} is the total liquid volume of the expansion tank, V_E is the thermal expansion volume, and V_O is the operating volume. Using the previously determined values for V_E and V_O, V_{Tot} is calculated to be 19.71 gallons.

5 PIPES AND FITTINGS

The piping and fittings of the demineralized cooling circuit must functionally compliment the equipment and materials they support. Surface ship electronic cooling water systems which use demineralized water as the cooling medium must

fabricate the cooling circuit from copper-nickel alloys, bronze, or corrosion-resistant steel (CRES) materials [7].

As the application of this cooling system exists in a marine environment, the likelihood for an electrolytic fluid, such as seawater or chloride-contaminated liquids, to interact with cooling circuit materials increases. The liquid contaminant can originate from various sources such as atmospheric condensation, heat exchanger tube failure, external system leakage, and piping insulation. It creates an environment that fosters and accelerates corrosion. Therefore, the following assessments assume that seawater or a chloride-contaminated liquid interacts with the cooling circuit's components, as is the case with most marine applications.

The causes and effects of galvanic corrosion, general corrosion, impingement attack, pitting corrosion, crevice corrosion, erosion-corrosion, and stress corrosion cracking on the viable cooling circuit materials were considered in the final design selection. Galvanic corrosion is mitigated through the use of materials with relatively similar surface potentials and low anode-to-cathode interface ratios to meet the corrosion rate limit of 0.009 mm/yr [13]. The effects of erosion corrosion are tempered by restricting liquid flow velocities to within the safe operating limits for the given internal piping diameters. The recommended maximum safe flow velocities for copper-nickel 90/10 and 70/30 are listed in Table 3 and [9]. The values from Table 3 are derived by [14] and are arranged by alloy and nominal pipe size (NPS). The use of demineralized water, selective build materials, piping geometry, and adherence to water chemistry specifications disrupts the mechanisms for other corrosion processes, as detailed by [6].

An analysis of material properties and the requirements of [15] determined that copper-nickel 90/10 is the most suitable material for construction of the demineralized water cooling circuit. Other permissible cooling circuit materials should concede to the use of copper-nickel 90/10 as the predominant build material. The need for a cathodic protection system when using copper-nickel alloys is limited or unnecessary based on the anticipated corrosion compatibility of materials and use of demineralized water. Further analysis is required to validate the need of a cathodic protection system should other materials be employed or another cooling medium be selected.

Table 3. Recommended safe maximum flow velocities

Alloy	$NPS \leq 3$	$NPS > 3$
Copper-nickel 90/10	2-3 *m/s*	3-3.5 *m/s*
Copper-nickel 70/30	2.5-3.5 *m/s*	3.5-4 *m/s*

6 WATER CHEMISTRY EQUIPMENT

6.1 Corrosion Analysis

Consideration is given to the effect corrosion has on cooling system components and its possible curtailment of the overall system lifespan. Design choices, enabled by military standards, mitigate the negative effects of corrosion mechanisms. However, they rely on robust administrative programs and technician follow-through to ensure that proper operation and maintenance are conducted.

Pourbaix diagrams for the permissible construction materials were used to evaluate the general corrosion resistance of the metals. They provide a basis of expectation for the passivity of metals in various conditions. The diagrams characterize the relationship between a metal's potential, measured by a reference electrode, and the pH of the liquid. They provide no information on the actual corrosion rate, nor do they give consideration to localized corrosion.

Superimposed Pourbaix diagrams developed by [16] were used determine the appropriate pH range to maintain the alloys' protective oxide layer. Maintaining the oxide layer is a key enabler of corrosion resistance. The superimposed diagram of copper and nickel determined that the predominant oxide layers for copper-nickel 90/10 and 70/30 alloys provide passivity at neutral to mildly alkaline values of pH. For a similar range, the iron and chromium diagram projects the that the oxide layers of Stainless Steel 304 and 316 alloys will also provide passivity to the base metal.

From this analysis, the water chemistry for the demineralized water should be maintained within the identified pH range to enhance the corrosion resistance properties of the system. The pH can be achieved and maintained with chemical additions or installed filters. However, chemical additions should minimize changes in conductivity, total dissolved solids, and chemicals deleterious to the construction materials. Challenging the effort of maintaining pH is the ionization of carbon dioxide to carbonic acid, and subsequently to bicarbonate and hydronium ions. The increased concentration of hydronium ions lowers the pH of the liquid, which makes it more acidic and prone to corrosion. Though the demineralized water may start out at a pH of 7 when freshly produced or demineralized, exposure to the carbon dioxide in the air can reduce pH to about 4.8 and should therefore be mitigated.

The minimum water chemistry standards required for the cooling system's demineralized water are derived by [7] and shown in Table 4.

Table 4. Demineralized Water Purity Requirements

Total Dissolved Solids	< 10 ppm
Chloride Concentration	≤ 0.065 elm
Oxygen Concentration	≤ 0.5 ppm
Conductivity	≤ 2 µmho/cm
Particulate Size	≤ 0.5 µm

The total dissolved solids (TDS) specification refers to the amount of organic or inorganic material dissolved in the cooling liquid. Examples of dissolved material include, but are not limited to, metals, salts, biomass, and chemical pollutants. An increase in TDS directly accelerates impingement attack, erosion-corrosion, and pitting; it could also indicate the presence of deleterious constituents such as mercury, chlorides, and such.

The chloride specification of 0.065 equivalents per million (elm) is equal to 0.25 grains of sea salt per gallon, or 4.3 ppm TDS. Chlorides for stainless steel and coppernickel alloys induce localized breakdown and dissolution of the protective oxide layer. Furthermore, chlorides migrate to the newly exposed pits and crevices to maintain their charge neutrality. The concentration of chlorides in these localized regions form a highly corrosive and acidic internal electrolyte.

An increase in oxygen concentration, external or internal to the cooling system components, exacerbates various corrosion mechanisms. As little can be done to change the oxygen concentration in the surrounding environment, the cooling system design focuses on minimizing the oxygen concentration within the bulk cooling solution. Vent valves are strategically installed on components and piping to allow the venting of trapped air and the release of liquid-entrained gasses. Additionally, an air eliminator near the suction of the pump, to which the return header and expansion tank piping are attached, provides similar capabilities. The device is located near the pump suction as it is nominally the system's lowest point of pressure. At this location, the solubility of noncondensing gasses is the lowest, which facilitates gasses coming out of the solution [5].

Conductivity measures the ion content of the bulk fluid. The analysis provides an insight into what other contaminants may be in the fluid aside from chlorides. For example, if an unintentional air addition was suspected, an increase in conductivity would be expected from the ionization of carbon dioxide to bicarbonate and hydronium ions. A pH analysis could also aid in detecting an air addition, as pH is expected to lower with the formation of carbonic acid. The conductivity analysis is not limited to this example but demonstrates how it can be used to detect a change in ion content from the baseline concentration and determine if hazardous constituents are present.

6.2 Chemistry Station and Filters

Filters and demineralizers mitigate the severity of water chemistry casualties and promote the health and longevity of the cooling system against corrosion. Filters remove the particulate content from the bulk fluid to protect pump bearings and valve seats, and prevent the build-up of matter in flow-restricting passages. Two filters are designed for use in the cooling system. One filter is installed on the return header, upstream of the pump's suction. Its purpose is to remove particulates from the return header prior to directing it to vulnerable downstream components. The second filter is installed in-line and upstream of the demineralizer as seen in Fig. 5. Its purpose is to prevent the early exhaustion or damage of the resin bed, as a filter in this location is more readily replaced and maintained than the demineralizer.

The demineralizer is designed as a recirculation loop about the pumps. It draws its suction at the discharge of the pumps, and its return is connected near the pump's suction. The demineralizer shall be capable of filtering the entire contents of the liquid cooling system within a 24-hour period with a 20% margin. A flow regulating device shall be used to maintain the required rate of coolant flow to the demineralizer. Excessive flow could damage the demineralizer components, whereas insufficient flow may not provide adequate filtering needs. An oxygen cartridge is the first component in the demineralizer. It houses an anion resin designed to remove oxygen from the bulk fluid. The second cartridge is a mixed-bed resin, made up of anions and cations, designed in-line and downstream of the first cartridge. The mixed-bed resin is designed to remove metallic particles, hard water ions, and carbon dioxide. The filter and demineralizer shall be selected to maintain the chemistry specifications listed in Table 4.

7 COLD PLATE DESIGN

Initial cold plate designs were based on the work done by [4], in which a single-pass serpentine arrangement and a counter-flow-style heat exchanger were assessed (Fig. 9). The heat removal performance of the counter-flow design enabled a lower maximum temperature per semi-conductor. This was in part due to each semi-conductor being exposed to multiple loops with lower maximum water temperatures. Other notable discussions are that the counter-flow heat exchanger required less pumping power due to less flow resistance from shorter pipe lengths with fewer bends. Additionally, diminishing returns in semi-conductor temperature decrease were observed at water velocities

greater than 2.5 m/s for the finalized cold plate tube diameter of 3/8".

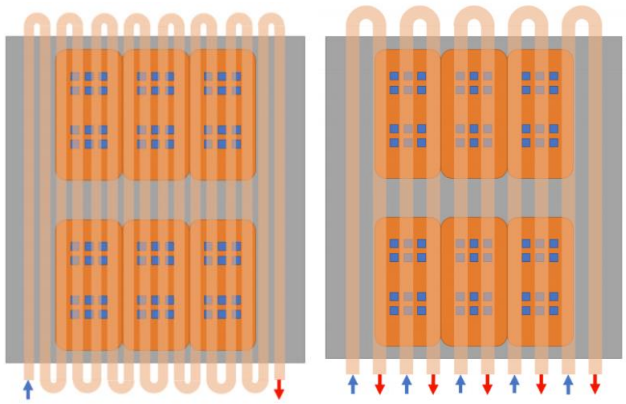

Figure 9. (a) Cold plate arranged as a single-pass heat exchanger, (b) Cold plate arranged as a counter-flow heat exchanger. © 2022 IEEE. Reprinted, with permission, from [4].

Several design iterations were assessed to optimize flow performance, thermal distribution, spacial footprint, and operational compatibility with interfacing systems. The final design iteration, Fig. 10, uses a single inlet, single outlet, opposing parallel flow design. It utilizes a plenum bridging segment to reduce the amount of required piping and introduced cooling water from both sides of the cold plate. Flow from the inlet piping, attached to the side of the cold plate, directs water into a 1" diameter plenum. In the inlet plenum, some of the flow is directed into 3/8" alternating channels, while the remainder continues to flow along the plenum to the back of the cold plate. The water reaching the back of the cold plate is directed along the back side, along a bridging segment, to a secondary inlet plenum on the opposite side of the cold plate. Water in this second inlet plenum is directed into its respective 3/8" alternating channels. Water continues along the 3/8" channels to their opposing sides' 1" diameter outlet plenums. Flow from the 3/8" channels originating from the second inlet plenum is directed to the back of the cold plate via the outlet plenum. The water reaching the back of the cold plate is directed along the back side, through a bridging segment, to an outlet plenum that reintegrates water originating from each inlet plenum. Water then exits the cold plate via the outlet piping, on the opposite side of the cold plate from the inlet piping. The inlet and outlet piping are located near the back end of the iPEBB and in concentric alignment with the axis of a hinge mechanism.

Previous design iterations required the use of flexible rubber hoses to permit lateral movement of the cold plates. In the latest design iteration, the cold plate securing mechanism was finalized to a hinge-style design that would pivot along the back edges of the iPEBB. Placement of the inlet and outlet piping at the center of rotation removed the need for the lateral movement of the cold plate and the use of flexible rubber hoses.

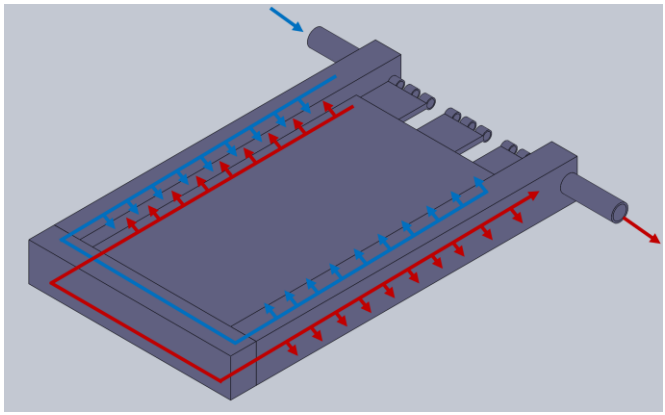

Figure 10. Cold plate arranged as a counter-flow heat exchanger.

A fluid simulation was performed on the final cold plate design. The simulation assumed a demineralized water inlet pressure of 100 lbf/in^2 and a mass flow rate of 0.5245 kg/s, or 336 gpm divided equally among the 40 cold pates at $46^{\circ}C$. The simulation results project that maximum flow velocities are to be well within the safe limits for the cold plate's internal channels. Additionally, model calculations forecast a pressure drop of approximately 0.2159 lbf/in^2 for the cold plate, which meets the required design criteria of ≤ 10 lbf/in^2 pressure loss across the component [7].

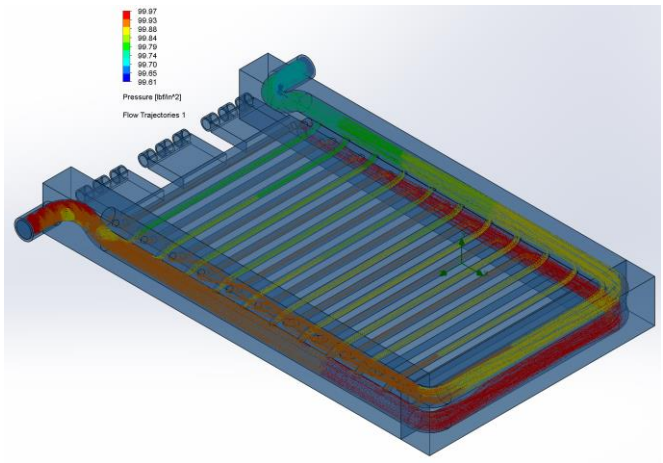

Figure 11. Cold plate demineralized water flow pressures.

8 FUTURE WORK

There were three significant topics discovered in the process of this research which require further study. The topics

discussed are not all-inclusive, but pose a significant challenge to the component and system architecture.

Variations in ship-wide NiPEC cooling system architectures should be evaluated. The number of cooling components required to support four corridors, with 12 compartments per corridor, denotes unwieldy operational and maintenance aspects under the current assumptions. This study developed a fully feasible system for a single NiPEC compartment. However, ship-wide implementation requires investigation into zonal cooling, super-loop, or other distributive cooling methods. The method could take advantage of the economies of scale while meeting the technical criteria addressed in this study. Additionally, this study did not address cooling system survivability, monitoring, safety, and control systems that are required for shipboard use and operator manageability.

iPEBB electrical isolation should be addressed and contained within the boundaries of the iPEBB. Given the large voltage capabilities of the iPEBB, electrical potentials permitted to travel outside the iPEBB shell could cause significant damage to equipment or personnel. Arcing across components, the electrolysis of the cooling liquid, accelerated corrosion, and other challenges multiply outside the bounds of the iPEBB. Electrical isolation can be equally, if not more, difficult to manage outside the iPEBB. Furthermore, [5] states that electrical isolation and grounding should not be achieved via piping systems.

A thermal design criterion required of the iPEBB, and not currently addressed, is that it must be able to operate at full power within its temperature parameters for at least 8 hours at an ambient temperature of 35 °C with no new supply of cooling water [7]. iPEBB cabinet cooling could provide a back-up means of addressing this requirement and should be considered in accordance with specifications of [17].

9 CONCLUSION

This study summarizes a first-pass design of a NiPEC liquid cooling system detailed by [6]. Each element of the cooling system has been investigated, relevant standards and requirements have been documented, and recommendations have been made for the candidate problem. Theoretical calculations and computer simulations presented validate the concept that indirect liquid cooling of the iPEBB is possible and can be used for heat loads not capable of being managed by convective air cooling. The groundwork has been set for initial and comprehensive NiPEC cooling system design possibilities. Various flow conditions can be explored and simulated by building upon the methodology and models. The accumulated literature in this study can guide on-going and future NiPEC cooling research. Prototyping and advanced modeling can develop more sophisticated means of cooling and can now be pursued.

ACKNOWLEDGEMENTS

This material is based upon research supported by, or in part by, the Office of Naval Research under award numbers ONR N00014-16-1-2945 Incorporating Distributed Systems in Early-Stage Set-Based Design of Navy Ships and ONR N00014-16-1-2956 Electric Ship Research and Development Consortium; and by the National Oceanic and Atmospheric Administration (NOAA) under Grant Number NA14OAR4170077 - MIT Sea Grant College Program.

Distribution A. Approved for public release, distribution is unlimited, DCN # 43-9716-22.

Any opinions, findings, conclusions or recommendations expressed in this paper are those of the authors and do not necessarily reflect the views of the U.S. Navy.

REFERENCES

[1] Rajagopal, N., DiMarino, C., Burgos, R., Cvetkovic, I., and Shawky, M., 2021, “Design of a high-density integrated power electronics building block (iPEBB) based on 1.7 kV SiC MOSFETs on a common substrate,” In 2021 IEEE Applied Power Electronics Conference and Exposition (APEC), IEEE, pp. 1–8.

[2] Petersen, L., Schegan, C., Ericsen, T. S., Boroyevich, D., Burgos, R., Hingorani, N. G., Steurer, M., Chalfant, J., Ginn, H., DiMarino, C., Montanari, G. C., Peng, F. Z., Chryssostomidis, C., Cooke, C., and Cvetkovic, I., 2022, “Power electronic power distribution systems (PEPDS),” *ESRDC Website, www.esrdc.com*.

[3] del Aguila Ferrandis, J., Chalfant, J., Cooke, C. M., and Chryssostomidis, C., 2019, “Design of a power corridor distribution network,” In 2019 IEEE Electric Ship Technologies Symposium (ESTS), IEEE, pp. 284–292.

[4] Padilla, J., Chalfant, J., Chryssostomidis, C., and Cooke, C., 2021, “Preliminary investigation into liquid-cooled PEBBs,” In 2021 IEEE Electric Ship Technologies Symposium (ESTS).

[5] MIL-HDBK-251, 2021, Reliability/design thermal applications, Department of Defense Handbook, January.

[6] Reyes, I., 2022, “Design and modeling of the Navy integrated power and energy corridor cooling system,” Master’s thesis, Massachusetts Institute of Technology.

[7] DOD-STD-1399, 2021, Cooling water for support of electronic equipment, Department of Defense Interface Standard, June Chapter 532, Revision A.

[8] Cooke, C., Chryssostomidis, C., and Chalfant, J., 2017, “Modular integrated power corridor,” In Electric Ship

Technologies Symposium (ESTS) 2017, IEEE, pp. 91–95.
[9] MIL-DTL-15730, 2021, Coolers, fluid, naval shipboard - hydrocarbon base oil and freshwater services, Department of Defense Detail Specification, June Revision N.
[10] Neutrium, 2012, Pressure loss from fittings - excess heat (k) method.
[11] Serth, R. W., 2007, *Process Heat Transfer: Principles and Applications*, Academic Press, Burlington, MA.
[12] Lienhard IV, J. H., and Lienhard V, J. H., 2020, *A Heat Transfer Textbook*, Phlogiston Press, Cambridge, MA.
[13] MIL-STD-889, 2021, Galvanic compatibility of electrically conductive materials, Department of Defense Standard Practice, 7 Revision D.
[14] Francis, R., 2016, Copper alloys in seawater: Avoidance of corrosion, Tech. rep., Copper Development Association Inc.
[15] MIL-STD-777, 2018, Schedule of piping, valves, fittings, and associated piping components for naval surface ships, Department of Defense Standard Practice, February Revision F.
[16] McCafferty, E., 2010, *Introduction to Corrosion Science*, Springer New York, New York, NY.
[17] MIL-DTL-2036, 2019, Enclosures for electric and electronic equipment, naval shipboard, Department of Defense Detail Specification, June Revision E.

BIOGRAPHIES

LT Ivan Reyes, USN, is a recent graduate of the Massachusetts Institute of Technology, with a Master's degree in Mechanical Engineering and Naval Architecture. He will be returning to the Fleet as an Engineering Duty Officer serving at the Puget Sound Naval Shipyard and Intermediate Maintenance Facility.

Dr. Julie Chalfant, Ph.D., is a research scientist at MIT Sea Grant. Her current areas of research include ship design and integration, including early-stage ship design tools and power and cooling systems. As a former active duty officer in the U.S. Navy, she also has significant experience in operating and maintaining Navy ships. She receved her Ph.D. from the Massachusetts Institute of Technology.

Prof. Chryssostomos Chryssostomidis, Ph.D., was educated at King's College, University of Durham, UK, and the Massachusetts Institute of Technology (MIT) Cambridge, MA, USA. He joined the MIT faculty in 1970 and retired in 2017. During his 47 years at MIT he served in various positions including Head of the Department of Ocean Engineering and Director of the MIT Sea Grant College Program. Professor Chryssostomidis is a Fellow Life Member of Society of Naval Architects and Marine Engineers. He was awarded the Captain Joseph H Linnard Prize for his paper submission to the Transactions of the Society of Naval Architects and Marine Engineers.